



ELSEVIER

Journal of Contaminant Hydrology 49 (2001) 87–109

www.elsevier.com/locate/jconhyd

JOURNAL OF
Contaminant
Hydrology

Effective parameters for two-phase flow in a porous medium with periodic heterogeneities

B. Ataie-Ashtiani^a, S.M. Hassanizadeh^{b,*}, M. Oostrom^c,
M.A. Celia^d, M.D. White^c

^a *Department of Civil Engineering, Sharif University of Technology, Iran*

^b *Hydrology and Ecology Section, Faculty of Civil Engineering and Geosciences, and Centre for Technical Geoscience, Delft University of Technology, PO Box 5048, 2600 Delft, GA, Netherlands*

^c *Environmental Technology Division, Pacific Northwest National Laboratory, USA*

^d *Department of Civil Engineering, Princeton University, Princeton, USA*

Received 20 April 2000; received in revised form 7 November 2000; accepted 8 November 2000

Abstract

Computational simulations of two-phase flow in porous media are used to investigate the feasibility of replacing a porous medium containing heterogeneities with an equivalent homogeneous medium. Simulations are performed for the case of infiltration of a dense nonaqueous phase liquid (DNAPL) in a water-saturated, heterogeneous porous medium. For two specific porous media, with periodic and rather simple heterogeneity patterns, the existence of a representative elementary volume (REV) is studied. Upscaled intrinsic permeabilities and upscaled nonlinear constitutive relationships for two-phase flow systems are numerically calculated and the effects of heterogeneities are evaluated. Upscaled capillary pressure–saturation curves for drainage are found to be distinctly different from the lower-scale curves for individual regions of heterogeneity. Irreducible water saturation for the homogenized medium is found to be much larger than the corresponding lower-scale values. Numerical simulations for both heterogeneous and homogeneous representations of the considered porous media are carried out. Although the homogenized model simulates the spreading behavior of DNAPL reasonably well, it still fails to match completely the results from the heterogeneous simulations. This seems to be due, in part, to the nonlinearities inherent to multiphase flow systems. Although we have focussed on a periodic heterogeneous medium in this study, our methodology is applicable to other forms of heteroge-

* Corresponding author. Tel.: +31-15-278-7346; fax: +31-15-278-5915.

E-mail address: majid@ct.tudelft.nl (S.M. Hassanizadeh).

neous media. In particular, the procedure for identification of a REV, and associated upscaled constitutive relations, can be used for randomly heterogeneous or layered media as well. © 2001 Elsevier Science B.V. All rights reserved.

Keywords: Effective parameters; Two-phase flow; Heterogeneous porous media; Upscaling; Capillary pressure–saturation curve

1. Introduction

The study of nonaqueous phase liquid (NAPL) transport in groundwater requires a correct description of multiphase flow in porous media. Such a description involves a number of material-dependent parameters, including relationships between capillary pressure, saturation, and relative permeability (P^c-S-k^r) relationships. These relationships are highly nonlinear and their determination is often a difficult task. This task is made even more difficult when the material under study is heterogeneous. One of the major difficulties in defining multiphase flow properties is the presence of small-scale heterogeneities, where different geologic materials may occur over a length scale of centimetres to tens of centimetres. Such length scales correspond to the size of common measuring devices, such as laboratory pressure cells, and to the typical size of cores taken at field sites. Therefore, identification of material properties at this scale is in principle possible. The measured properties, including the nonlinear functional relationships, can vary widely over this length scale. Such variability can significantly affect overall flow properties of the system, including such factors as the spreading behavior of non-aqueous liquids. These heterogeneities can also produce localized pools of NAPL.

While the detailed structure of the porous medium governs the overall behavior of the system, for most practical purposes the detailed fluid distribution in such a medium is not of interest. Rather, we are commonly interested in more global measures and assessments of the NAPL movement. Also, even if we choose to resolve the system at the small scale, it is currently computationally infeasible to discretize a compositional multiphase model at such small scales. Furthermore, even if a detailed numerical model is constructed and run, it is virtually impossible to obtain data for all of these heterogeneities for a large domain. Thus, we are motivated to derive effective properties that incorporate the influences of small-scale heterogeneities and can be employed in an equivalent homogenous model of the porous medium applied at length scales larger than the individual heterogeneities.

Considerable work has been directed at the problem of upscaling permeabilities for single-phase flow. These works have been reviewed recently in papers by Wen and Gomez-Hernandez (1996) and Renard and de Marsily (1997). The techniques for upscaling saturated permeability range from the simple averaging of heterogeneous values within an averaging block to sophisticated inversions, after the solution of the flow equation at the measurement scale within an area surrounding the block. All techniques have their own advantages and limitations. It is now understood that upscaled permeabilities depend on the geometry and properties of the fine-scale permeabilities, the boundary conditions imposed on the region to be upscaled, and the discretisation

pattern used in the numerical flow model. Approximations based on assumptions such as structured heterogeneity and periodic boundary conditions lead to more general upscaling relations (Miller et al., 1998).

Upscaling of constitutive relations for multiphase flow is significantly different from that for single-phase flow due to inherent nonlinearities. Upscaling of the intrinsic permeability in a multiphase flow system, without upscaling of P^c-S-k^r relations, has been done. For example, Durlofsky et al. (1997) have applied a flexible grid method to upscale the permeability in a multiphase flow system while a single P^c-S-k^r relation was assumed for the whole medium. There is a significant literature on the upscaling issues in petroleum engineering. Fayers and Hewett (1992) give a general review of the trends of scaling problems in petroleum reservoir simulation. A more recent review is given by Christie (1996), and a critical review of pseudofunctions for upscaling relative permeabilities is presented by Barker and Thibeau (1997). Formally exact methods for upscaling two-phase flow problems are not available. Two main approaches can be identified: upscaling through use of representative elements of volume (Haldorsen, 1986) and complete renormalization (King, 1989; King et al., 1993). In fact, the upscaling through representative elements of volume approach is really a form of renormalization in which the reservoir description is viewed as composed of a number of regions which are classified into types. In the renormalization method, the focus is on using a fast approximate method to determine average properties for much smaller units of volume than those of the representative elements of volume concept. But, in this case, the averaging is performed consistently for every renormalization element in the reservoir (Fayers and Hewett, 1992).

Amazine et al. (1991) have developed a homogenisation approach and applied it to the case of two-phase transient flow in periodically heterogeneous media. They have assumed constant-shape P^c-S-k^r relationships for the domain. Desbarats (1995) investigated the upscaling of capillary pressure–saturation relationships under static conditions of capillary gravity equilibrium. The averaging regions are horizontal layers, parallel to the phreatic surface, as in one-dimensional models of infiltration. They did not consider any upscaling of relative permeability–saturation curves. Honarpour et al. (1995) examined upscaling of both capillary pressure and relative permeability curves, and observed that small-scale layering and laminations present in sandstone cores produced significant capillary effects that affected the oil recovery behavior. In these and many similar studies (see the review articles referenced above for additional examples), the main conclusion is that upscaling two-phase flow properties remains a difficult task for which additional research is needed. Overall, the study of the literature reveals that general approaches for upscaling of P^c-S-k^r relations still need to be developed.

In the present work, the feasibility of replacing a medium containing heterogeneities with an equivalent homogeneous medium is studied. The main question is whether the mean spreading behaviour of NAPL in a heterogeneous medium can be reproduced with the aid of the equivalent homogeneous medium. In order to focus on specific aspects of the problem, we have considered rather simple heterogeneity patterns here. In particular, we have constructed two periodic heterogeneous porous media, for which the average saturated permeability and P^c-S-k^r relations are computed. The scale at which

effective parameters may be defined is determined based on the concept of a representative elementary volume (REV). The REV defines the 'larger scale' and is used to compute upscaled constitutive relationships, based on high-resolution simulations that incorporate the small-scale heterogeneities.

Numerical simulations are carried out for both heterogeneous and homogeneous representations of the considered porous medium. The simulations are conducted with the water–oil mode of the multi-fluid flow simulator STOMP (White and Oostrom, 1997). Processes modeled in STOMP and its numerical features are described in Section 2. In Section 3, STOMP is used to simulate a laboratory experiment on DNAPL infiltration. The results are compared to two other model simulations of this experiment. This exercise serves as verification of STOMP's ability to simulate heterogeneous systems, and also provides insights into proper boundary condition specification for certain two-phase flow problems. In Section 4, two periodic heterogeneous porous media are defined and their characteristics are specified. In Section 5, the infiltration event of a DNAPL in these two systems is simulated taking into account the details of heterogeneity. In Section 5, the procedure for upscaling properties of a heterogeneous medium is described and the equivalent homogeneous medium is defined. In Section 6, results of simulations of the DNAPL infiltration event, using the homogeneous description of the system, are presented and compared with the detailed simulation results. Finally, conclusions are presented in Section 7.

Although we focus on a periodic heterogeneous medium in this study, our methodology is applicable to other forms of heterogeneous media. In particular, the procedure for the identification of a REV can be used for randomly heterogeneous or layered media as well.

2. Numerical model

The numerical simulator Subsurface Transport Over Multiple Phases (STOMP) (White and Oostrom, 1997) is used herein to simulate two-phase flow in porous media. STOMP is a package consisting of 11 modes for simulation of non-isothermal multi-phase flow and multi-component transport in a heterogeneous medium in three dimensions. This fully implicit, integrated finite difference code has been used to simulate a variety of multi-fluid systems (e.g. Oostrom and Lenhard, 1998; Schroth et al., 1998; Oostrom et al., 1997). The simulations discussed in this paper were conducted with a non-hysteretic two-phase version of the water–oil mode of STOMP. In this mode, the following mass balance equations for the water (superscript w) and oil (superscript o) phases are solved:

$$\frac{\partial}{\partial t} (n \rho_\gamma S_\gamma) = - \nabla \mathbf{q}_\gamma \text{ for } \gamma = w, o. \quad (1)$$

In addition, the multiphase version of Darcy's equation is used:

$$\mathbf{q}_\gamma = - \frac{\rho_\gamma k_{r\gamma} \mathbf{k}}{\mu_\gamma} (\nabla P_\gamma + \rho_\gamma g \mathbf{z}_g) \text{ for } \gamma = w, o. \quad (2)$$

In these equations, n is porosity, ρ is the density (ML^{-3}), S is the saturation, \mathbf{q} is the fluid flux ($\text{ML}^{-2} \text{T}^{-1}$), k_r is the relative permeability ($-$), \mathbf{k} is the intrinsic permeability tensor (L^2), μ is the viscosity ($\text{ML}^{-1} \text{T}^{-1}$), P is the pressure ($\text{ML}^{-1} \text{T}^{-2}$), g is the gravitational acceleration (LT^{-2}), \mathbf{z}_g is the unit vector assumed positive in the vertical direction, subscript γ corresponds to the aqueous (w) or nonaqueous (o) phase.

In addition to the well-known Van Genuchten (1980) or Brooks and Corey (1964) capillary pressure–saturation relations, this version of the simulator also allows for tabular input of fluid saturations and pressures to define the constitutive relationship between capillary pressure and saturation. Relative permeability–saturation relations are interpolated from tabular input or computed based on either the Burdine (1953) or Mualem (1976) pore-size distribution model. To accommodate the type of upscaling studies performed herein, the code has been modified to allow for directionally (x , y , and z) dependent relative permeability–saturation relations, in addition to the traditional scalar version of these relationships.

3. Model verification

In this section, we demonstrate the applicability of the STOMP model to heterogeneous media and test its ability to simulate a multi-fluid laboratory experiment. The simulated experiment is described fully by Kueper et al. (1989). In this experiment, tetrachloroethylene (PCE) infiltrates into a sand pack composed of layers of four different kinds of sand. The configuration of the assembled sand lenses is shown in Fig. 1. Table 1 gives sand properties including permeability and Brooks–Corey parameters (Brooks and Corey, 1964) of the PCE–water drainage capillary pressure curve. These are best-fit parameter values that were obtained by Kueper et al. (1989) by matching the Brooks–Corey model to experimental data.

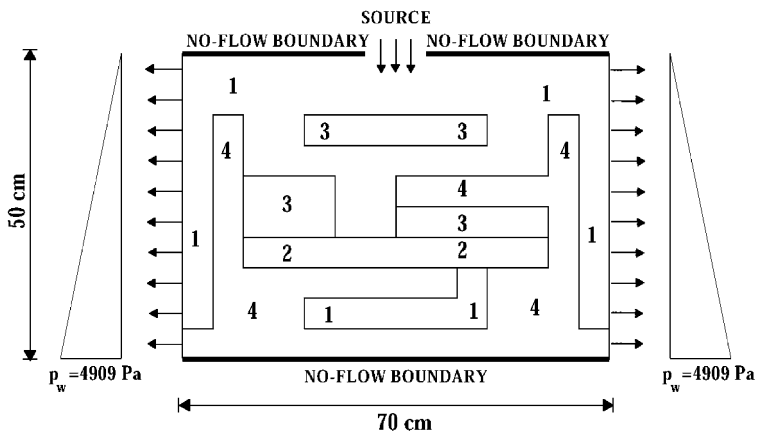


Fig. 1. Configuration and boundary conditions for simulation of PCE infiltration in a flow tank (after Kueper et al., 1989).

Table 1
Properties of sands used by Kueper et al. (1989)

	Units	Sand 1	Sand 2	Sand 3	Sand 4
Permeability k	[m ²]	5.04×10^{-10}	2.05×10^{-10}	5.62×10^{-11}	8.19×10^{-12}
Porosity n	[-]	0.4	0.39	0.39	0.41
Entry pressure p_d	[m]	0.0377	0.0377	0.0377	0.1350
Pore size distribution index λ	[-]	3.86	3.51	2.49	3.30
Residual saturation S_{wr}	[-]	0.078	0.069	0.098	0.189

At the beginning of the experiment, dyed PCE was released into the initially water-saturated sand. The source area at the center of the top of the sand pack was subjected to a constant head of 4 cm of PCE, which is equal to a fluid pressure of 640 Pa. The PCE has a density of 1630 kg m⁻³ and a viscosity of 0.90×10^{-3} Pa s. The PCE propagation in time was visually recorded; no measurement of saturation within the medium was made. The experiment was simulated by Kueper and Frind (1991) using a finite element model. An acceptable match was found between experimental and simulated results when a constant PCE saturation of 0.38 was assumed at the PCE source. Helmig (1997) also simulated this experiment with a PCE saturation of 0.40 imposed at the source points.

In our simulations, we looked specifically into the influence of boundary conditions at the source on the resulting solutions. Two different sets of boundary conditions were employed there. The first set is similar to the boundary conditions used by Kueper and

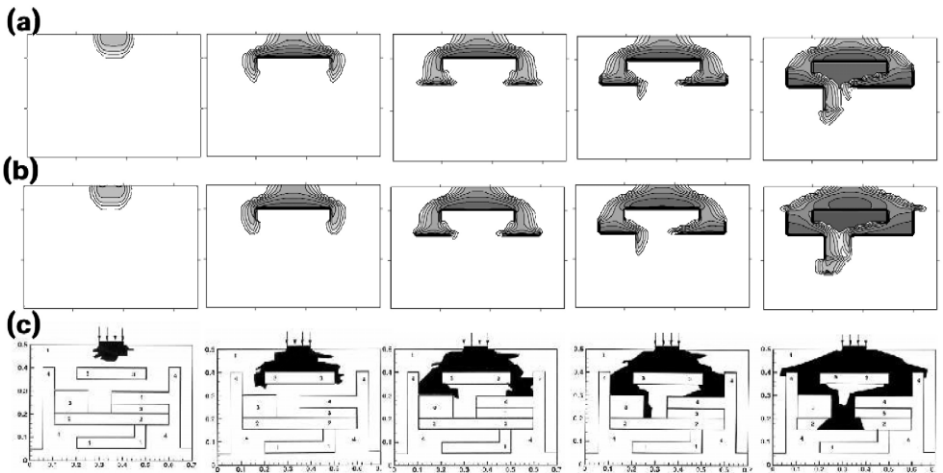


Fig. 2. (a) Observed distributions of PCE after 34, 126, 184, 220, 313 s; (b) simulated distribution of TCE after 30, 130, 180, 220, 310 s with Dirichlet B.C. for DNAPL and zero-flux B.C. for water at source nodes; (c) simulated distribution of PCE after 30, 130, 180, 220, 310 s with Dirichlet B.C. for both PCE and for water at source nodes.

Frind (1991) and Helmig (1997), resulting in a constant saturation condition at the source boundary. This was achieved by imposing Dirichlet boundary conditions: a constant PCE pressure of 640 Pa (equal to 4 cm of NAPL) for non-wetting phase and a constant pressure of 213 Pa for water. This amounts to a capillary pressure, P_c , of 427 Pa corresponding to a PCE saturation of 39%. In the second set, the same boundary condition for PCE was employed (a constant pressure of 640 Pa) but a zero-flux boundary condition was used for water. Boundary conditions for the remainder of domain boundaries are shown in Fig. 1. The domain was discretized using a constant nodal spacing of 1.25 cm in both horizontal and vertical directions. A time step of 10 s was used throughout the simulation.

Fig. 2 illustrates the distribution of fluids in the sand pack at various times based on experimental and numerical results. As is evident, the agreement between experimental and numerical values is reasonable. Comparison of the last two figures in Fig. 2a,b, and c shows that the second boundary condition set (with zero flux for water) yields a somewhat better match with experimental results. Further evidence of the superiority of

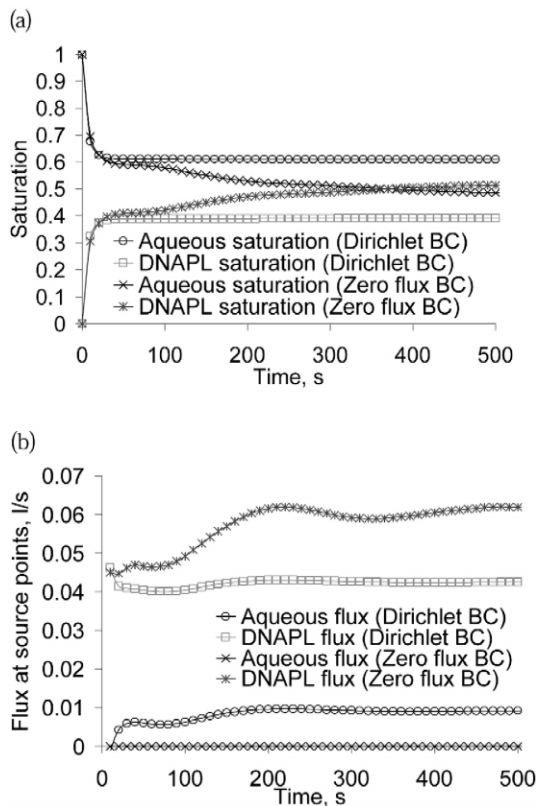


Fig. 3. (a) Aqueous and PCE saturation in the node below the source. (b) Aqueous and PCE fluxes at source points.

the zero-flux boundary condition is illustrated in Fig. 3, where the PCE saturation at one of the nodes below the source and the aqueous and DNAPL fluxes at source points are plotted. The plots show that application of the Dirichlet boundary condition in the numerical simulation leads to a flux of water into the medium through the PCE source area. This is not a correct result as in the experiment only PCE infiltrated into the medium. Therefore, the second set of boundary conditions is physically more realistic and appears to give somewhat better results. Overall, this exercise gives us confidence in the applicability of STOMP simulator to heterogeneous porous media of the kind that is investigated in the rest of this manuscript, while demonstrating the potential importance of boundary condition specification in DNAPL infiltration problems.

4. Definition of test cases

In this section, we define two heterogeneous porous media to be used in our upscaling procedure. We are not considering the case of large-scale heterogeneities, which should be modeled explicitly in any flow simulation. Our focus is on heterogeneities with a small correlation length, which are amenable to upscaling and homogenization. In this work, we consider two periodic media: a straight pattern (porous medium P-1) and a staggered pattern (porous medium P-2). The two media are illustrated in Fig. 4. These particular patterns of heterogeneity are chosen for their simplicity. Our main goal is not to investigate the influence of various types of heterogeneity but to test our upscaling procedure. Therefore, we prefer to avoid introducing complications due to intricate heterogeneity patterns. Moreover, very similar patterns have been considered in other upscaling studies (see e.g. Amazine et al., 1991; Durlafsky, 1991; Bourgeat and Hidani, 1995) and by authors who apply mathematical homogenization techniques (see e.g. Beliaev and Kozlov, 1993; Panfilov, 1998). Thus, our numerical results may be used for comparison purposes in evaluating the results of homogenization theories.

The hypothetical porous media P-1 and P-2 have dimensions and properties comparable to the sand tank used in the Kueper et al. experiment. The white background in Fig. 4 is coarse-grained sand while the black areas designate fine-grained sand. The properties of the coarse-grained sand are the same as Sand 1 in Kueper et al. (1989), whereas the properties of the fine-grained sand are a combination of Sands 3 and 4. Pertinent sand properties, including permeability and Brooks–Corey parameters of the PCE-water main-drainage capillary pressure curve, are listed in Table 2. Fluid properties of PCE are the same as those given in the pervious section.

The computational domain (Fig. 4) was discretized using a constant nodal spacing of 1.25 cm in both horizontal and vertical directions. A time step of 10 s was used throughout the simulation. The maximum number of Newton iterations was 32, with a convergence factor of 10^{-6} . Upwind interfacial averaging was used for PCE and water relative permeabilities. Harmonic averages were used for all other flux components.

In the simulations, PCE is released into initially water-saturated sand. The PCE source area is 10 cm long and is at the center of the top boundary (see Fig. 4). A constant PCE-flux of 3.15×10^{-4} m/s is uniformly assigned to the source area. Our

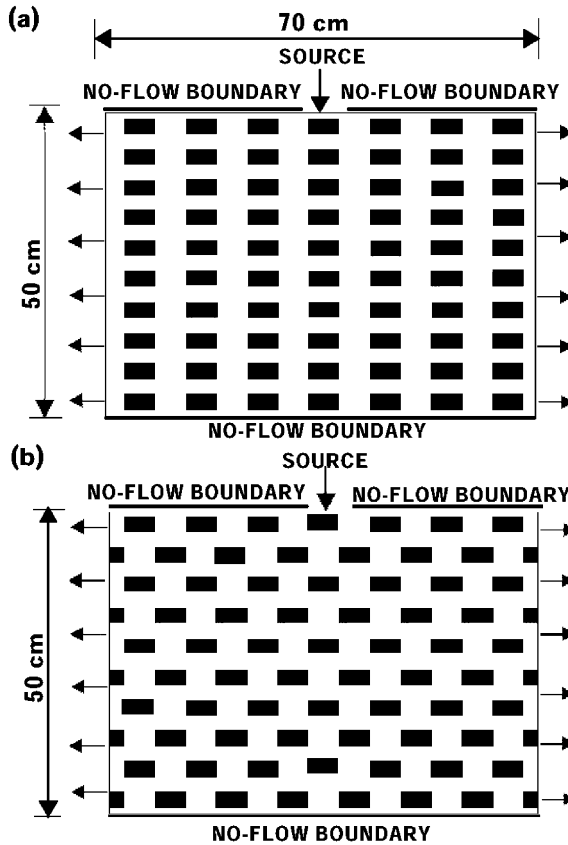


Fig. 4. Two periodic patterns of heterogeneity: (a) P-1 and (b) P-2. The white background is coarse-grained sand while the black areas designate fine-grained sand.

choice of boundary condition guarantees that the amount of DNAPL infiltrating the medium will be the same for all cases. Thus, differences in the distribution of DNAPL, calculated for different cases, will be due only to choices in soil properties and not due to the source boundary conditions. In this section, results of numerical simulations based on actual characteristics of the medium are presented and discussed.

Table 2
Properties of sands used in upscaling simulations

Property	Units	Coarse-grained sand	Fine-grained sand
Permeability k	[m ²]	5.0×10^{-10}	5.0×10^{-11}
Porosity n	[-]	0.4	0.4
Entry pressure p_d	[m]	0.0377	0.1350
Pore size distribution index λ	[-]	3.86	2.49
Residual saturation S_{wr}	[-]	0.078	0.098

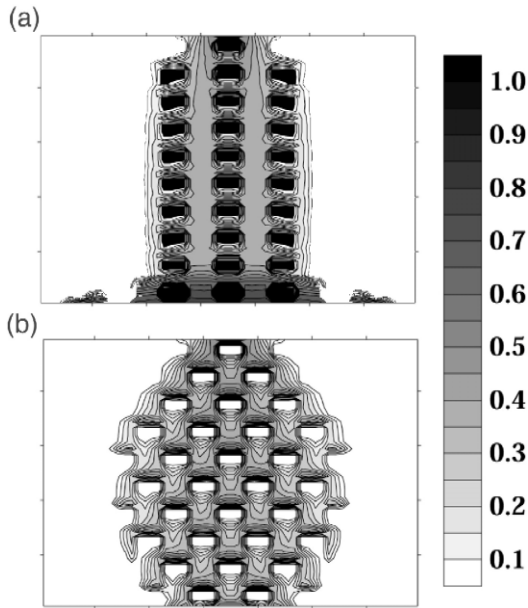


Fig. 5. Simulated PCE saturations after 500 s for (a) pattern P-1 (upper graph), and (b) pattern P-2 (lower graph). The assigned porous medium properties for the coarse- and fine-grained sand are listed in Table 2.

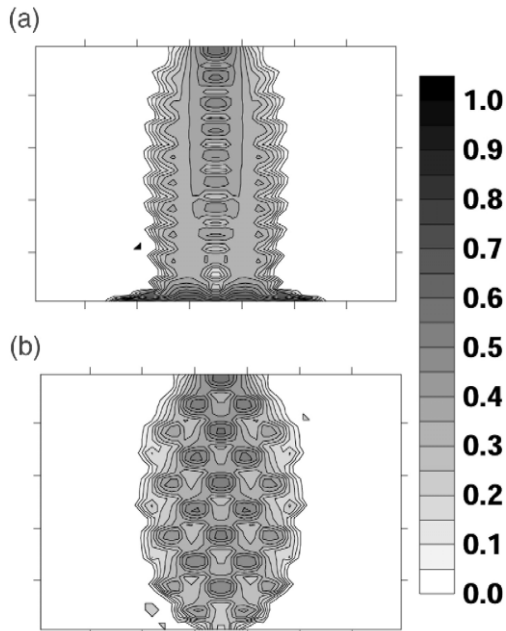


Fig. 6. Simulated PCE saturations after 500 s for (a) patterns P-1 (upper graph) and (b) pattern P-2 (lower graph) when coarse-grained sand multiphase parameters were assigned to the fine-grained sand. Both sands maintained their actual permeability values.

Fig. 5 shows the distribution of the PCE plume for the two porous media configurations, P-1 and P-2, after 500 s of infiltration. As seen in this figure, the PCE saturation distribution is quite different for the two cases, due to the difference in heterogeneity patterns. The horizontal spreading of PCE is larger in the P-2 medium than in the P-1 medium. This is because in the staggered pattern, fine sand blocks cause pooling of PCE and force it to move horizontally. Differences in both the saturated permeabilities and the two-phase flow parameters contribute to the differences in flow patterns. This latter observation is based on the next series of simulations, where we have assumed that fine-grained sand has the same P^c-S-k^r relations as the coarse-grained sand while maintaining its own intrinsic permeability value. Fig. 6 illustrates the PCE saturation distribution for this case in patterns P-1 and P-2 at 500 s. Obviously, differences between Figs. 5 and 6 are due to the influence of heterogeneity in the P^c-S-k^r relations. Comparison of the two figures shows that when heterogeneities in constitutive relationships are ignored, less spreading of PCE is observed. The effect is most significant in the fine sand. It is seen from Fig. 5 that in these simulations, PCE saturation remains zero in the fine media when P^c-S-k^r effects are included. This is because the capillary pressure at the fine sand surface remains below the entry pressure of PCE for this material. Ignoring the P^c-S-k^r effects of fine sand, however, results in PCE entering the fine sand as seen in Fig. 6.

5. Upscaling of two-phase flow parameters

For the calculation of upscaled permeabilities and constitutive relationships, we need to identify representative domains for patterns P-1 and P-2. This was achieved by applying the concept of a representative elementary volume (REV). Results of simulations with actual properties (Fig. 5) were used to determine whether a REV could be defined. The procedure is as follows. Consider the saturation distribution of medium P-2 at 500 s (Fig. 5b). At every nodal point, the PCE saturation is averaged over an averaging volume, centered at that point, and the result is assigned to that nodal point. Contours of averaged DNAPL saturation obtained with seven different averaging sizes are plotted in Fig. 7a–i. The smallest averaging block has a size of 3×3 grid elements and the largest is 17×17 . The black border indicates the area where no average saturation can be defined; the width of the black border is equal to half the averaging domain length. Obviously, simulations with the homogenized media will lack the local details obtained with the heterogeneous simulations. This is evident in Fig. 7 where local effects become less and less distinguishable as the averaging domain size is increased. For example, for the averaging domain of 9×9 elements (center figure) and larger, local pools are not easily recognizable, although they have not fully vanished.

Fig. 8 shows the plot of averaged PCE saturation as a function of the averaging area, at three different points: within the coarse sand (solid squares), within the fine sand (open squares), and at their boundary (solid triangles). The graphs resemble the typical graphs given for the definition of a REV (see e.g. Bear, 1972). Here, however, the fluctuations in average saturation do not die off completely even for an averaging size as large as half the domain size. This is, we believe, due to the fact that the length scale of

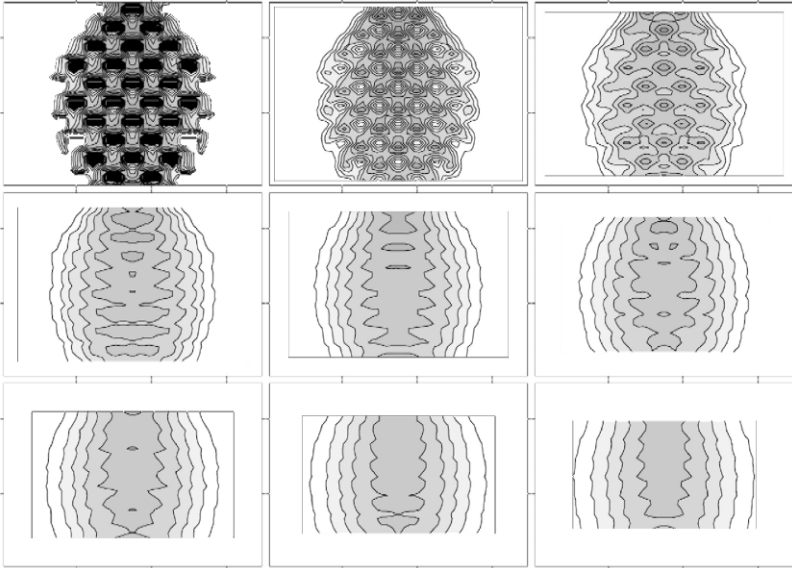


Fig. 7. Contours of average PCE saturations at $t = 500$ s obtained with averaging domain sizes of 1×1 , 3×3 , 5×5 , 7×7 , 9×9 , 11×11 , 13×13 , 15×15 and 17×17 elements, from left to right and from top to bottom, respectively. Note that the black border indicates the area where no average saturation can be defined. The width of this border is equal to half the averaging block size.

heterogeneities is not small compared to the source size, which is the length scale of the spreading process. Thus, strictly speaking, one cannot identify a proper REV here. However, the amplitude of these fluctuations reduces to a negligible amount in the early part of the graph. Therefore, based on results of Fig. 8, a block of 10×10 cm is considered to be an appropriate REV and is employed for homogenization of constitutive properties of the medium in this work. Corresponding representative blocks for

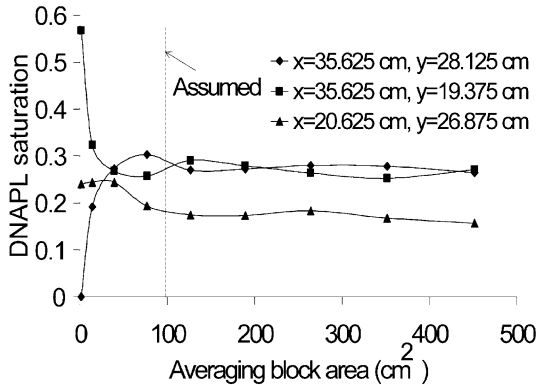


Fig. 8. Variation in PCE saturations after 500 s in domain P-2 vs. averaging block area.

patterns P-1 and P-2 are shown in Fig. 9. Note that their size equals the size of periodicity of the two patterns, which we might expect given the structural regularity of the heterogeneity.

Next, average permeabilities and constitutive relationships for our representative blocks were calculated numerically. The procedure is as follows. A unidirectional flow of both water and PCE is established across a block. This is achieved by applying, at the block faces perpendicular to the flow direction, a constant pressure P^{nw} for PCE and a constant pressure P^w for the aqueous phase. The difference $P^c = P^{nw} - P^w$ is chosen to be the same at both ends, which means that the same capillary pressure exists at the boundaries. The pressure differences across the block, ΔP^w and ΔP^{nw} , are kept at a value of 100 Pa for both fluids in all simulations. This corresponds to a pressure gradient comparable to that observed in the main medium (Fig. 5). Meanwhile, no-flow boundary conditions are imposed on the block faces parallel to the flow. Simulations for a given P^c are carried out until apparent equilibrium is reached. Average saturation and directional k^r -values are then calculated for the block. After equilibrium conditions have been reached, P^c is increased incrementally up to 10,000 Pa (holding $\Delta P^w = \Delta P^{nw} = 100$ Pa) and the procedure is repeated for every new P^c . Fig. 10 shows the imposed water, DNAPL, and capillary pressures on the top of REV blocks. In this fashion, constitutive relationships are obtained for each block in two different directions.

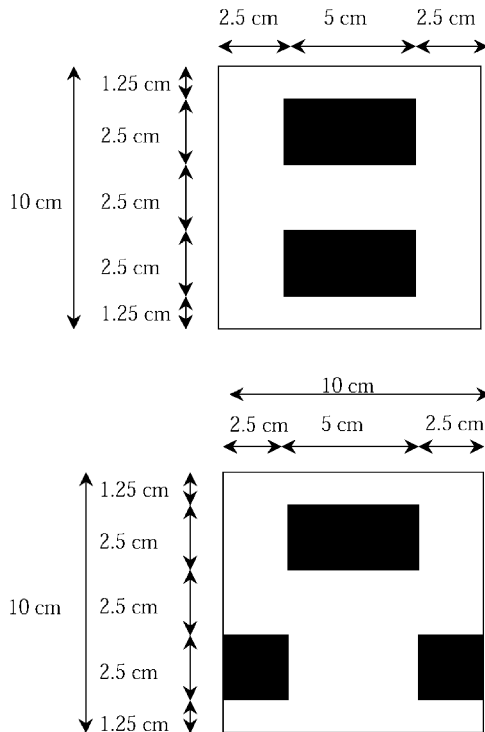


Fig. 9. Considered elementary blocks (REV) for patterns (a) P-1 (upper figure) and (b) P-2 (lower figure).

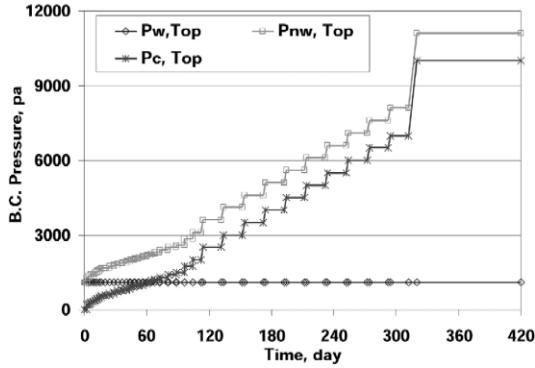


Fig. 10. Imposed water, PCE and capillary pressures on the REV block.

Obviously, for calculating intrinsic permeability, only single-phase flow is simulated. The saturation distributions in the P-1 block for different P^c 's are shown in Fig. 11. The plots demonstrate the variation of saturation in various regions of the fine and coarse sand in response to the imposed capillary pressure at the boundaries. The results indicate that, even when the imposed P^c at the boundaries is 1500 Pa, which is more than the entry pressure of 1325 Pa, PCE cannot penetrate the finer-grained sand blocks. This is because the relative permeability of coarse-grained sand to water is reduced to zero and thus the water remains entrapped in the finer-grained material.

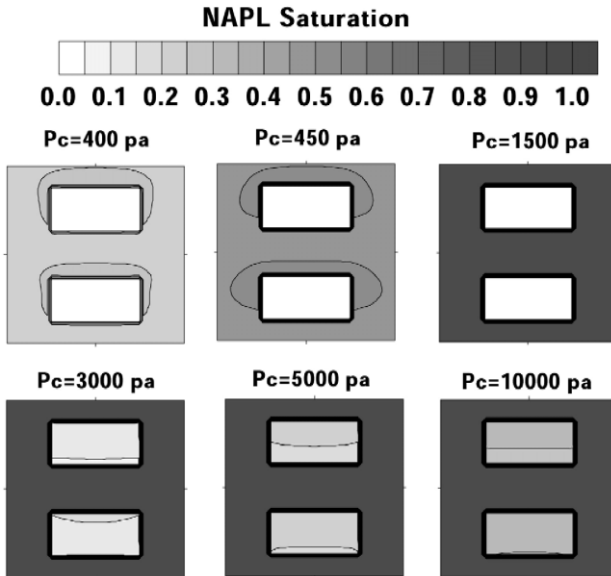


Fig. 11. Saturation distribution within a representative P-1 block for different capillary pressures.

Fig. 12 gives P^c-S-k^r curves for the two sands (fine and coarse) and the homogenized curves for the two blocks. As seen, the upscaled constitutive relationships are distinctly different from the corresponding curves for fine and coarse sands. It is evident that a simple arithmetic averaging of properties of the two sands cannot represent the homogenized situation. The residual saturation is significantly larger for the equivalent

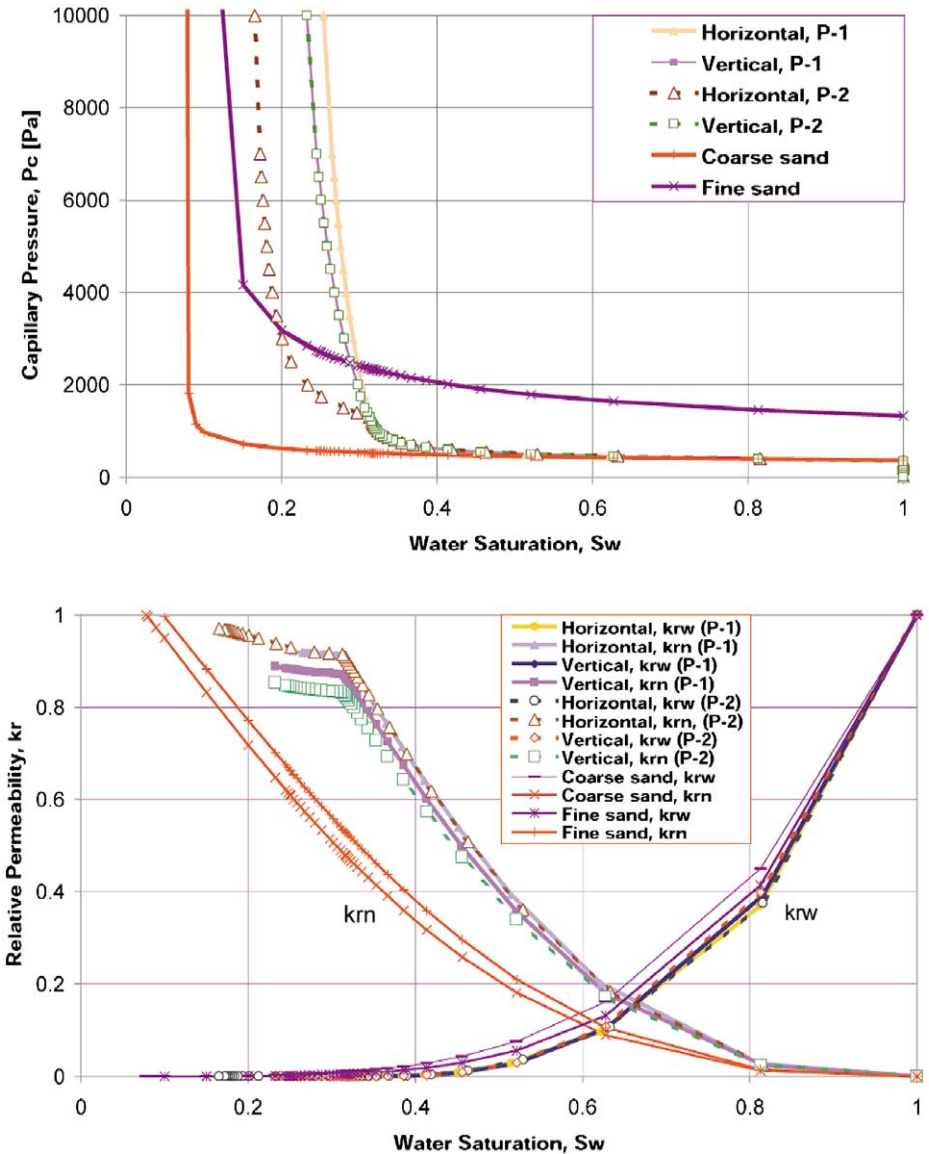


Fig. 12. P^c-S-k^r relations for the elementary blocks.

medium. From Fig. 12a, one may conclude that the upscaled P^c-S curves are almost the same for both patterns. For the most part there is little directional dependence. There is a discrepancy for the P^c-S curves of pattern P-2 in the horizontal direction. This is a numerical artifact that is caused by the interplay of the fine material with Dirichlet boundary conditions. When flow is in the horizontal direction, the fine sand in pattern P-2 will be in contact with the inflow boundary. As a result, it will be fully saturated with PCE as soon as the boundary P^c exceeds entry pressure of fine sand. But when 1-D flow is established in the vertical direction, the coarse sand may reach its residual water saturation (and thus no permeability to water) and cause the entrapment of water inside the fine material. These results are consistent with those of Ferrand and Celia (1992), who used a pore-scale network model to analyze P^c-S curves for similar patterns of heterogeneity.

The upscaled relative permeability curves are significantly different from those of fine and coarse sands. More significantly, they are directional dependent. This is in contrast with the common assumption that relative permeability is a scalar property. This dependency is not because of boundary condition effects; it is observed even before PCE enters the fine sand. This appears to be a general characteristic of heterogeneous media. It is consistent with the stochastic results of Yeh et al. (1985), who showed that the anisotropy ratio (horizontal/vertical) of effective conductivity is a function of mean capillary pressure or mean moisture content. A similar result was obtained by, among others, Braun et al. (1998) for a stratified porous medium.

6. Simulations with effective two-phase flow parameters

In this section, results of simulations with homogenized two-phase flow parameters are presented and discussed. Obviously, such results do not show the kind of detail in the saturation distribution that was shown in Fig. 5. Thus, they should not be compared directly with results of the detailed simulations, but instead with the averages of the saturation distribution such as those presented in Fig. 7.

In replacing the heterogeneous medium with an equivalent homogeneous medium, one has a number of choices. One choice is to ignore the presence of fine sand blocks and assume that the medium is homogeneous with properties similar to that of the coarse-grained sand. Another choice would be to include the effect of saturated permeability of the fine-grained sand but ignore its two-phase flow characteristic. A third alternative is to include both permeability and two-phase flow effects. All three alternatives are simulated here. The averaged saturation distribution and results of various simulations are presented in Figs. 13 and 14, for patterns P-1 and P-2, respectively. In each figure, results of five different simulations, as described below, are given.

- Graphs R1 show the average of saturation distributions depicted in Fig. 5, where all heterogeneity details are included (see Section 5). The saturation distributions shown in Fig. 5 are averaged over representative blocks of size 10×10 cm (as depicted in Fig. 8), following the procedure described in Section 5. Note that the black border indicates the area where no average saturation can be defined. The width of this border is equal to half the averaging block size.

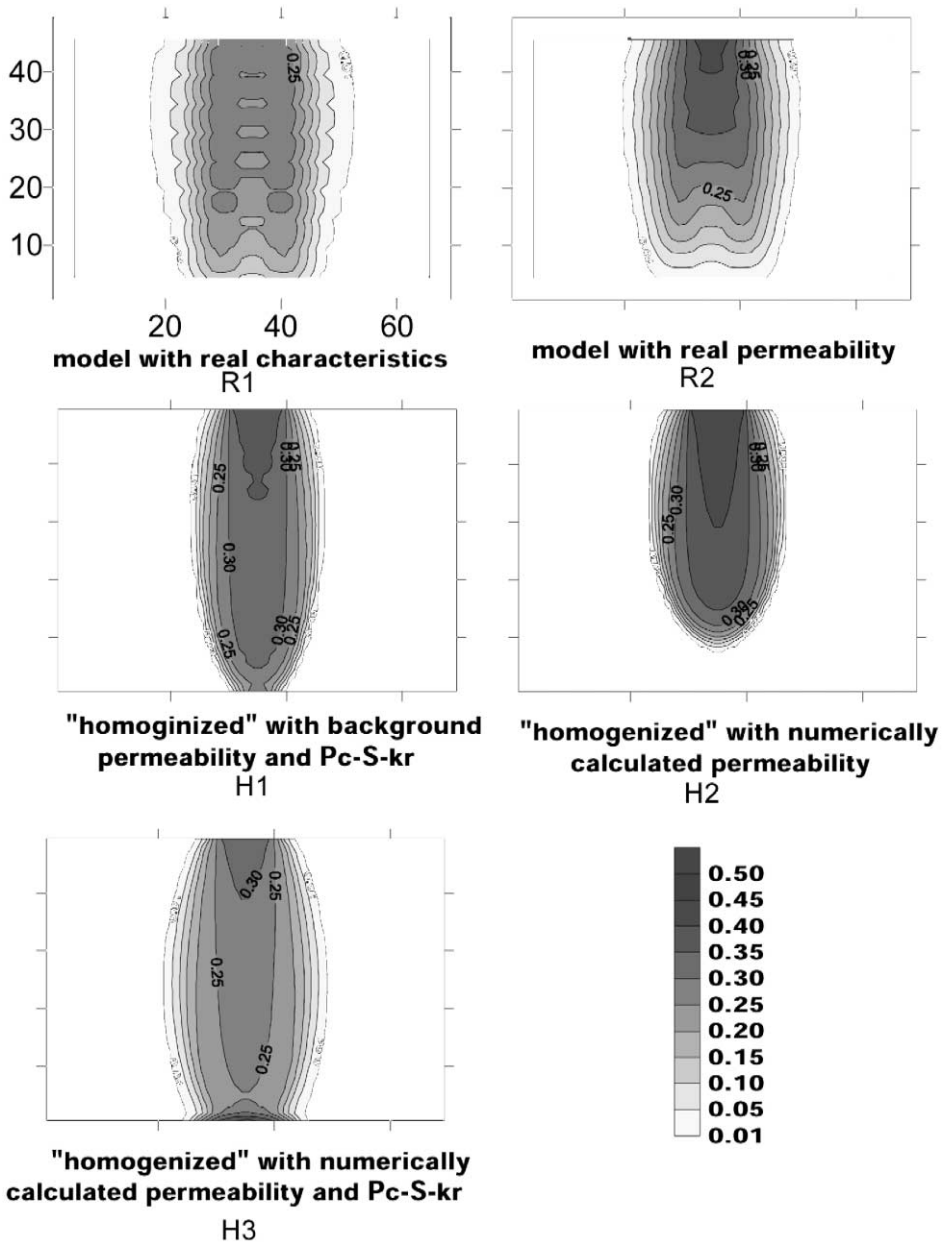


Fig. 13. PCE saturations after 310 s for pattern P-1. Results are shown for R1, R2, H1, H2 and H3 cases.

- Graphs R2 show the average of saturation distributions depicted in Fig. 6, where heterogeneity in intrinsic permeability is included but two-phase flow properties of coarse-grained sand are used for both sands (see Section 5). Here too, the saturation

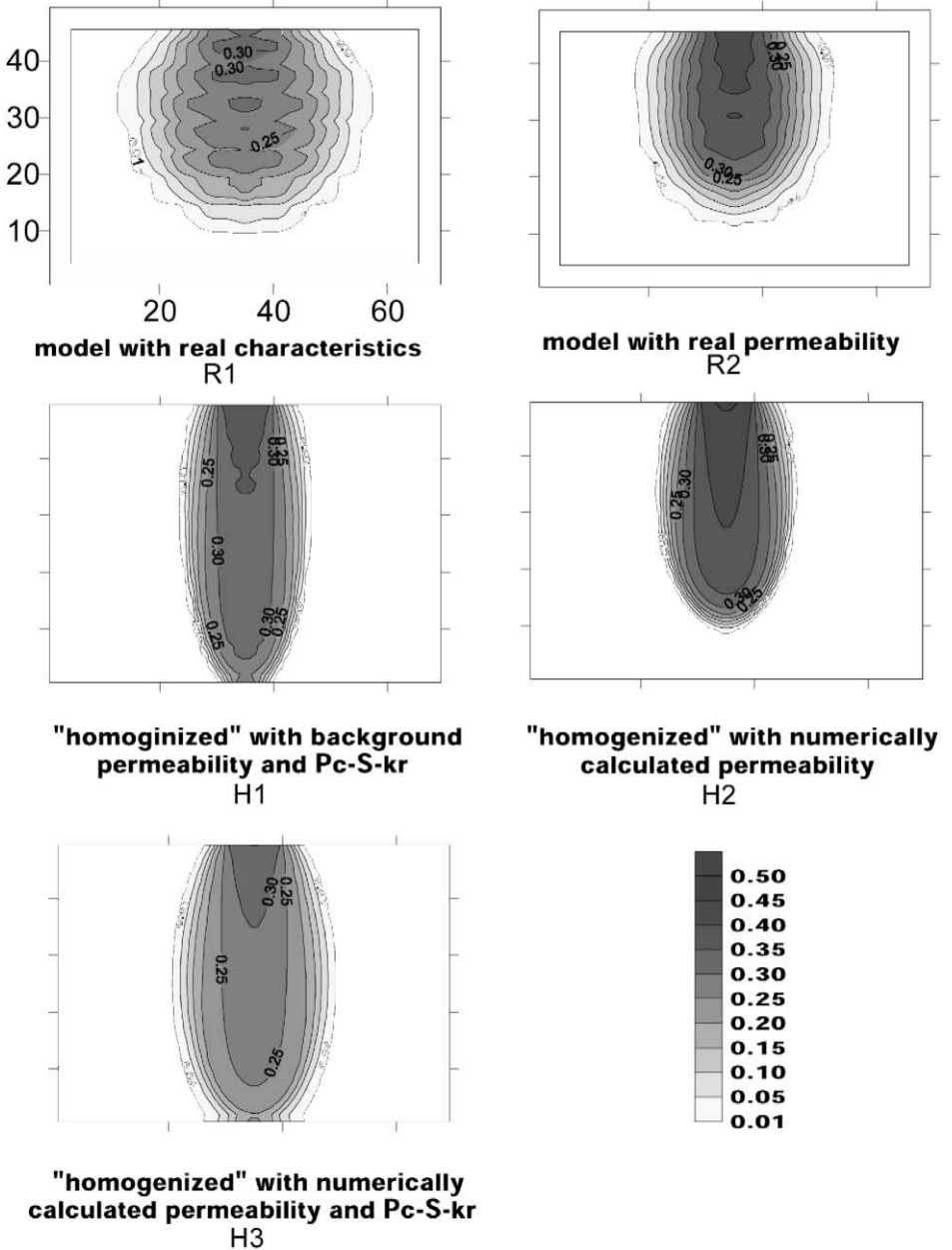


Fig. 14. PCE saturations after 310 s for pattern P-2. Results are obtained for cases R1, R2, H1, H2 and H3.

distributions shown in Fig. 6 are averaged over representative blocks of Fig. 8, following the procedure described in Section 5.

- Graphs H1 show results of “homogenized” simulations where permeability and constitutive relationships of coarse-grained sand are used for both sands. In other words, the presence of fine-grained sand blocks is completely neglected.
- Graphs H2 show results of “homogenized” simulations with numerically calculated average permeability for the medium and with two-phase flow parameters of coarse-grained sand used for both sands.
- Graphs H3 show results of homogenized simulations with numerically calculated average permeability and with upscaled two-phase flow parameters obtained in Section 6. As explained earlier, there is little directional dependency for upscaled P^c – S curves, thus the results of vertical cases have been employed here. However, the directional dependency of k^r – S curves have been considered in these simulations.

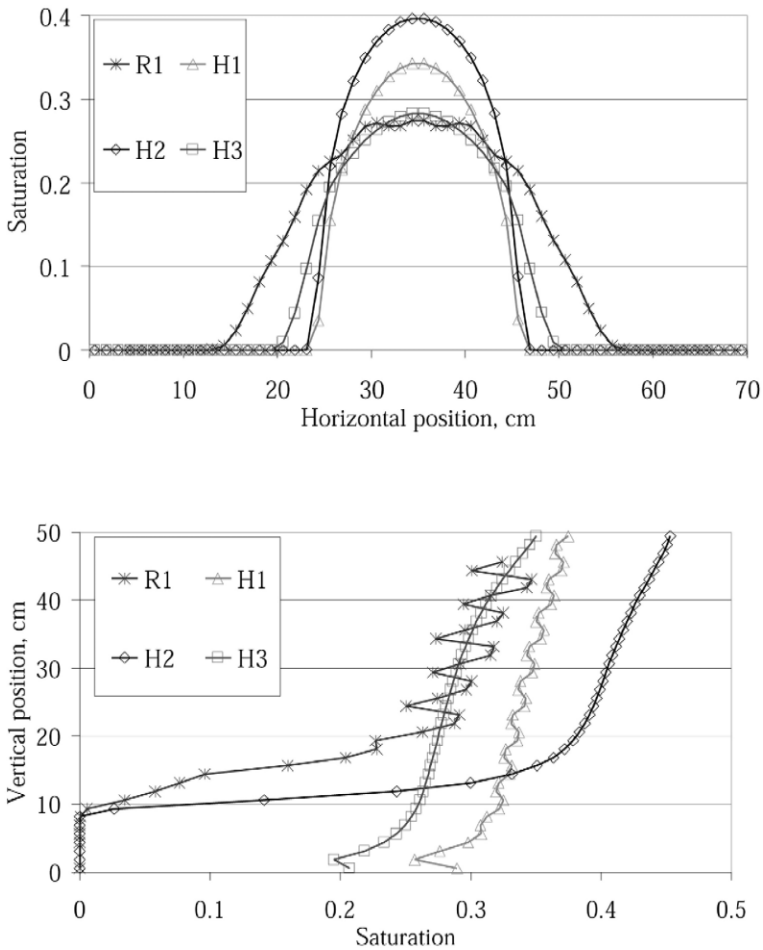


Fig. 15. PCE saturations after 310 s for pattern P-2 at the horizontal and vertical centerlines for cases R1, H1, H2 and H3.

Graphs R1 are viewed as representing the actual average behavior of our system and other graphs are compared to them. First, consider graphs R1 and R2. Although the forms of saturation contours are similar, the maximum saturation in R2 is much higher. This is the same result that was observed in Figs. 5 and 6 and was discussed in Section 5. A comparison of graphs H1 and R1 shows that if the presence of heterogeneities is ignored, completely wrong results will be obtained. Neither the form of the saturation contours nor the maximum saturation in H1 is anywhere close to those in R1. A similar conclusion is drawn from comparing graphs R1 and H2: it is evident that accounting for heterogeneity of saturated permeability is not enough. Finally, comparing all graphs, one may conclude that graph H3, where heterogeneities in both permeability and two-phase flow parameters are included, does a better job in mimicking the “real” saturation distribution in R1, especially for pattern P-1 (Fig. 11). Although the “real” saturation distribution cannot be reproduced exactly in any of the cases, the larger saturation contours (25% and 30%) agree reasonably well in H3 and R1. Fig. 15 shows the PCE saturation at the horizontal and vertical centerlines of the medium with pattern P-II. This figure also confirms that the H3 case gives better results and can capture the spreading of PCE better than other cases. The main discrepancy for R1 and H3 is near the lower boundary. In H3, the PCE front reaches the bottom faster than that in case R1. The pooling is an artifact due to the front reaching the bottom boundary. Obviously, the choice of comparison criteria is dependent on the problem of interest. One may use other criteria such as the immobile saturation, the total flux of DNAPL passing a given surface, the extent of the plume, or the total DNAPL in place. All in all, the agreement between results from the homogenized model and heterogeneous model may not be considered as completely satisfactory. The lateral spreading of PCE is underestimated by the homogenized model while the vertical extent is overestimated.

7. Summary and conclusions

Heterogeneities in soil properties have a significant influence on the spreading behavior of nonaqueous liquids in soil and groundwater. Also, the presence of small-scale lenses of fine-grained sand and/or clay may produce localized pools of NAPL after the spreading has stopped. However, for most practical purposes the detailed fluid distribution is not of interest. One is commonly interested in more global measures and assessments of the NAPL movement. In particular, for numerical simulations, it is often appropriate to replace the heterogeneous medium with an equivalent homogeneous medium. For this purpose, one has to define effective properties that incorporate the effects of small-scale heterogeneities. In this work, we have demonstrated the feasibility of replacing a medium containing heterogeneities with an equivalent homogeneous medium for the case of two-phase flow. Numerical simulations were carried out with the water–oil mode of multi-fluid flow simulator STOMP (White and Oostrom, 1997). The ability of STOMP to simulate heterogeneous media was verified through simulation of a laboratory experiment on DNAPL infiltration, described by Kueper et al. (1989). This simulation pointed out how different boundary condition specifications can influence DNAPL infiltration results.

For two periodic heterogeneous porous media, the upscaled saturated permeability and upscaled capillary pressure–saturation–relative permeability (P^c – S – k^r) relationships were computed. The scale at which effective parameters may be defined was determined based on the concept of representative elementary volume (REV). Upscaled capillary pressure–saturation curves were found to be distinctly different from the curves for individual regions of heterogeneity. In particular, the irreducible water saturation for the homogenized medium was found to be much larger than the corresponding lower-scale values. The k^r – S relation was found to be directional dependent and quite sensitive to the pattern of heterogeneity. This finding contradicts the common assumption that the relative permeability is a scalar value and independent of direction. This result is consistent with the stochastic results of Yeh et al. (1985), as they showed that the anisotropy ratio (horizontal/vertical) of effective conductivity is a function of mean capillary pressure or mean moisture content. A similar result was obtained by Braun et al. (1998) for a stratified porous medium. To simulate the homogenized case, the numerical model STOMP was modified to handle directional-dependence of k^r – S relation.

Numerical simulations were carried out for both heterogeneous and homogenized representations of the considered porous media. A homogenization of the intrinsic permeability, without taking into account the multiphase flow properties of the fine sand, did not provide acceptable results. In particular, the spreading pattern of PCE is not simulated well. The closest results to the detailed heterogeneous model were obtained with the fully homogenized model (with both intrinsic and multiphase flow properties upscaled). Nevertheless, the results are not completely satisfactory. In particular, the lateral spreading of PCE is underestimated and the vertical extent is overestimated. It is obvious that the upscaling of multiphase flow properties is not trivial. The nonlinearities inherent to multiphase flow are the main source of difficulty. Another very important issue is that in our simulations, we have assumed that the governing equations at lower and upper scales are exactly the same. This may be another source of disagreement between homogenized and heterogeneous simulation results. Thus, in addition to searching for more elaborate procedures for upscaling of the medium and flow properties, one should investigate the possible need for modification of the governing equations at the larger scale. For example, Panfilov (1998) has shown, through mathematical homogenization, that for a medium similar to P-2, the upscaled P^c – S relationship has to be replaced with a dynamic relationship. Similar modifications may be needed for other terms in the governing equations.

Although we have focussed on a periodic heterogeneous medium in this study, our methodology is applicable to other forms of heterogeneous media. In particular, the procedure for the identification of a REV can be used for randomly heterogeneous or layered media as well.

Acknowledgements

A 1-year Visiting Research Fellowship provided by the Delft University of Technology to B. Ataie-Ashtiani is greatly appreciated. Also, this work has been supported in

part by the NATO Scientific Affairs and Environmental Division under grant CRG950230, the U.S. National Science Foundation under grant EAR-9805376, the U.S. Department of Energy (DOE) under grant DE-FG07-96ER14703, and the Delft University of Technology through a Visiting Faculty appointment provided to M.A. Celia. Pacific Northwest National Laboratory is operated for DOE by Battelle Memorial Institute.

References

- Amazine, B., Bourgeat, A., Kobbe, J., 1991. Numerical simulation and homogenisation of two-phase flow in heterogeneous porous media. *Trans. Porous Media* 6, 519–547.
- Barker, J.W., Thibeau, S., 1997. A critical review of the use of pseudorelative permeabilities for upscaling. *SPE Reservoir Eng.* 12, 138–143.
- Bear, J., 1972. *Dynamics of Fluids in Porous Media*. American Elsevier, New York, NY, 764 pp.
- Beliaev, A.Yu., Kozlov, S.M., 1993. Hierarchical structures and estimates for homogenized coefficients. *Russ. J. Math. Phys.* 1, 5–18.
- Bourgeat, A., Hidani, A., 1995. Effective model of two-phase flow in a porous medium made of different rock types. *Appl. Anal.* 58, 1–29.
- Braun, C., Hassanizadeh, S.M., Helmig, R., 1998. Two-phase flow in stratified porous media: effective parameters and constitutive relationships. *Proceedings of the International Conference Computational Methods in Water Resources*, Crete, Greece, 15–19 June, 1998. pp. 43–50.
- Brooks, R.H., Corey, A.T., 1964. Hydraulic properties of porous media. *Hydrol. Pap.* 3, Civ. Eng. Dep., Colo. State Univ., Fort Collins.
- Burdine, N.T., 1953. Relative permeability calculations from pore-size distribution data. *Pet. Trans.* 198, 71–77.
- Christie, M.A., 1996. Upscaling for reservoir simulation. *J. Pet. Technol.* 48, 1004–1010.
- Desbarats, A.J., 1995. Upscaling capillary pressure–saturation curves in heterogeneous porous media. *Water Resour. Res.* 31, 281–288.
- Durlofsky, L.J., 1991. Numerical calculation of equivalent grid block permeability tensors for heterogeneous porous media. *Water Resour. Res.* 27, 699–708.
- Durlofsky, L.J., Jones, R.C., Milliken, W.J., 1997. A nonuniform coarsening approach for the scale-up displacement processes in heterogeneous porous media. *Adv. Water Resour.* 20, 335–347.
- Fayers, F.J., Hewett, T.A., 1992. A review of current trends in petroleum reservoir description and assessment of the impacts on oil recovery. *Adv. Water Resour.* 15, 341–365.
- Ferrand, L.A., Celia, M.A., 1992. The effect of heterogeneity on the drainage capillary pressure–saturation relation. *Water Resour. Res.* 28, 859–870.
- Haldorsen, H.H., 1986. Simulator parameter assignment and the problem of scale in reservoir engineering. In: Lake, L.W., Carroll, H.B. Jr. (Eds.), *Reservoir Characterization*. Academic Press, Orlando, FL, pp. 293–340.
- Helmig, R., 1997. *Multiphase Flow and Transport Processes in the Subsurface*. Springer-Verlag, Berlin.
- Honarpour, M.M., Cullick, A.S., Saad, N., Humphreys, N.V., 1995. Effect of rock heterogeneity on relative permeability: implications for scaleup. *J. Pet. Technol.* 47, 980–986.
- King, P.R., 1989. The use of renormalization for calculating effective permeability. *Transp. Porous Media* 4, 37.
- King, P.R., Muggeridge, A.H., Price, W.G., 1993. Renormalization calculations of immiscible flow. *Transp. Porous Media* 12, 237.
- Kueper, B.H., Frind, E.O., 1991. Two-phase flow in heterogeneous porous media: 1. Model development. *Water Resour. Res.* 27, 1049–1057.
- Kueper, B.H., Abbot, W., 1989. Experimental observations of multiphase flow in heterogeneous porous media. *J. Contam. Hydrol.* 5, 83–95.

- Miller, C.T., Christakos, G., Imhoff, P.T., McBride, J.F., Pedit, J.A., 1998. Multiphase flow and transport modeling in heterogeneous porous media: challenges and approaches. *Adv. Water Resour.* 21, 77–120.
- Mualem, Y., 1976. A new model for predicting the hydraulic conductivity of unsaturated porous media. *Water Resour. Res.* 12, 513–522.
- Oostrom, M., Lenhard, R.J., 1998. Comparison of relative permeability–saturation–pressure parametric models for infiltration and redistribution of a light nonaqueous phase liquid in sandy porous media. *Adv. Water Resour.* 21, 145–157.
- Oostrom, M., Hofstee, C., Dane, J.H., 1997. Light nonaqueous-phase liquid movement in a variably saturated sand. *Soil Sci. Soc. Am. J.* 61, 1547–1554.
- Panfilov, M., 1998. Up-scaling two-phase flow in double porosity media: non-uniform homogenization. In: Crolet, J.M., Hatri, M.E. (Eds.), *Recent Advances in Problems of Flow and Transport in Porous Media*. Kluwer Academic Publishing, Dordrecht, The Netherlands, pp. 195–215.
- Renard, Ph., de Marsily, G., 1997. Calculating equivalent permeability: a review. *Adv. Water Resour.* 20, 253–278.
- Schroth, M.H., Istok, J.D., Selker, J.S., Oostrom, M., White, M.D., 1998. Multifluid flow in bedded porous media: laboratory experiments and numerical simulations. *Adv. Water Resour.* 22, 169–183.
- van Genuchten, M.Th., 1980. A closed-form equation for predicting the hydraulic conductivity of unsaturated soils. *Soil Sci. Soc. Am. J.* 44, 892–898.
- Wen, X., Gomez-Hernandez, J.J., 1996. Upscaling hydraulic conductivities in heterogeneous media: an overview. *J. Hydrol.* 183, ix–xxxii.
- White, M.D., Oostrom, M., 1997. *STOMP, Subsurface Transport Over Multiple Phases. User’s Guide*. Pacific Northwest National Laboratory Report PNNL-11218.
- Yeh, T.-C., Gelhar, L.W., Gutjahr, A.L., 1985. Stochastic analysis of unsaturated flow in heterogeneous soils: 3. Observations and applications. *Water Resour. Res.* 21, 465–471.